Superconducting to Normal Phase Transition in Tantalum

WILLIAM B. ITTNER
International Business Machines Corporation, Poughkeepsie, New York
(Received March 26, 1958)

Measurements were made of the rate at which the superconducting phase collapses radially in a hollow cylindrical tantalum specimen following the sudden application of a longitudinal magnetic field greater than the critical field. The measured transition rates confirm the hypothesis that the propagation is controlled by electromagnetic damping associated with eddy currents generated in the normal phase. The results, moreover, may be interpreted on the basis of a theoretical treatment of the problem first published by Pippard, provided that suitable modifications are incorporated to include the thermal effects which accompany the transition.

I. INTRODUCTION

IT was proposed as early as 1936 that the propagation rate associated with the transition between the superconducting and normal phases of a metal is limited by the electromagnetic damping which accompanies the spatial propagation of the magnetic field within the normal material.[1,2] A theory describing the electromagnetic damping associated with the collapsing superconducting phase in a semi-infinite medium was developed by both Pippard[3] and Lifshitz.[4] Faber[5] extended this treatment to describe the propagation in a cylindrical medium and made detailed measurements on the radial contraction of the superconducting phase in cylindrical tin specimens. His results confirm, in most respects, the eddy current damping hypothesis for fields only slightly greater than the critical value, H_c.

Recent measurements with thin-walled hollow cylinders have shown, however, that for fields several times the critical value, the approximations made by Faber are not applicable. The experimental results are, moreover, in good agreement with the original predictions of Pippard. For tantalum, it is necessary to extend Pippard's work to include the effects of latent and eddy current heat which alter the transition rates in a manner first suggested by Faber.

II. THEORY

A. The Semi-Infinite Solid

Pippard has discussed this case in detail. The field distribution in the normal phase is specified by the equation

$$\frac{\partial^2 H}{\partial x^2}-\frac{4\pi}{\rho}\frac{\partial H}{\partial t}=0, \qquad (1)$$

where H is the field, ρ is resistivity, t is time, and x is distance. The equation must be solved subject to the following boundary conditions:

$$x=0,\quad t\geq 0,\quad H=H_0,$$

$$x=x',\quad t>0,\quad H=H_c,$$

$$x=x',\quad t>0,\quad \frac{\partial H}{\partial x}=-\frac{4\pi H_c\dot{x}'}{\rho}.$$

Here, H_0 and H_c denote the applied and critical magnetic fields, respectively, and x' represents the position of the interphase boundary which is parallel to the applied field and the yz plane.

Pippard has shown that

$$H=H_0-\frac{(H_0-H_c)}{\mathrm{erf}\lambda}\,\mathrm{erf}\left(\frac{x}{(\rho t/\pi)^{\frac{1}{2}}}\right), \qquad (2)$$

where λ is a solution of

$$\lambda\ \mathrm{erf}\lambda=\left(\frac{H_0}{H_c}-1\right)\frac{\exp(-\lambda^2)}{\sqrt{\pi}}. \qquad (3)$$

According to this result, the time required for the normal phase to propagate a distance x' is given by $t=\pi x'^2/\rho\lambda^2$. t thus decreases continuously with increasing field, H_0.

Faber has pointed out that this process is not an isothermal one but is accompanied by the absorption of latent heat at the moving interphase boundary and the dissipation of Joule heat by eddy currents within the normal phase. It is desirable to extend Pippard's results to include these thermal phenomena which will affect the transition by altering the boundary value of the critical field.

If one denotes by L the latent heat per cm^3 associated with the phase transition, heat will be absorbed at the rate $L\dot{x}'$ per cm^2 sec at the moving boundary. The thermal equations which specify the temperatures in the normal and superconducting regions are, respectively,

$$k_n\frac{\partial^2 T_n}{\partial x^2}=\frac{\partial T_n}{\partial t},\quad 0\leq x\leq x', \qquad (4)$$

[1] K. Mendelssohn and R. B. Pontius, Physica 3, 327 (1936).
[2] H. G. Smith and K. C. Mann, Phys. Rev. 54, 766 (1938).
[3] A. B. Pippard, Phil. Mag. 41, 243 (1950).
[4] E. M. Lifshitz, J. Exptl. Theoret. Phys. (U.S.S.R.) 9, 834 (1950).
[5] T. E. Faber, Proc. Roy. Soc. (London) A219, 75 (1953).

and

$$k_s\frac{\partial^2 T_s}{\partial x^2}=\frac{\partial T_s}{\partial t},\quad x>x', \tag{5}$$

where k_n and k_s denote the diffusivities of the two regions and T is temperature. These equations must be solved subject to the following boundary conditions[6]:

$$\begin{array}{lll} t=0, & x'=0, & T_s=0,\\ t=\infty, & x'=\infty, & T_n=0,\\ t>0, & x=0, & T_n=0,\\ t<\infty, & x=\infty, & T_s=0,\\ t>0, & x=x', & T_n=T_s,\\ t>0, & x=x', & K_n\partial T_n/\partial x-K_s\partial T_s/\partial x=-L\dot{x}'. \end{array}$$

K_n and K_s denote the thermal conductivities of the two regions. Solutions which satisfy the first four boundary conditions are

$$T_n=A\ \mathrm{erf}\left(\frac{x}{2(k_nt)^{\frac{1}{2}}}\right), \tag{6}$$

and

$$T_s=B\ \mathrm{erfc}\left(\frac{x}{2(k_st)^{\frac{1}{2}}}\right), \tag{7}$$

where $\mathrm{erfc}y=1-\mathrm{erf}y$.

Substituting Eqs. (6) and (7) into the last two boundary conditions and letting[7]

$$\epsilon_n=\frac{x'}{2(k_nt)^{\frac{1}{2}}}=\left(\frac{\rho}{k_n\pi}\right)^{\frac{1}{2}}\frac{\lambda}{2},$$

$$\epsilon_s=\frac{x'}{2(k_st)^{\frac{1}{2}}}=\left(\frac{\rho}{k_s\pi}\right)^{\frac{1}{2}}\frac{\lambda}{2},$$

we obtain

$$A\ \mathrm{erf}\epsilon_n-B\ \mathrm{erfc}\epsilon_s=0, \tag{8}$$

and

$$\frac{AK_n\exp(-\epsilon_n^2)}{(\pi k_nt)^{\frac{1}{2}}}+\frac{BK_s\exp(-\epsilon_n^2)}{(\pi k_st)^{\frac{1}{2}}}=-L\dot{x}'=-\frac{L}{2}\left(\frac{\rho}{\pi t}\right)^{\frac{1}{2}}\lambda. \tag{9}$$

Solving Eqs. (10) and (11) for A and B leads to an expression for the boundary temperature depression,

$$T'=\frac{-L\rho^{\frac{1}{2}}(\lambda/2)\ \mathrm{erfc}\epsilon_s\ \mathrm{erf}\epsilon_n}{[K_n\exp(-\epsilon_n^2)/\sqrt{k_n}]\ \mathrm{erfc}\epsilon_s+[K_s\exp(-\epsilon_s^2)/\sqrt{k_s}]\ \mathrm{erf}\epsilon_n}. \tag{10}$$

The mathematical treatment of the eddy current dissipation is considerably more complex since it involves the generation of heat which is distributed spatially within the volume of normal material. It is possible, however, to obtain a rough estimate of the effects of the eddy current heat in the following manner.

The total joule heat per unit volume per unit time is $j^2\rho$, where

$$j=-\frac{1}{4\pi}\frac{\partial H}{\partial x}=\frac{(H_0-H_c)}{4\pi x'}\frac{2}{\sqrt{\pi}}\frac{\lambda}{\mathrm{erf}\lambda}\exp(-\pi x^2/\rho t). \tag{11}$$

For λ less than unity (which is the case for driving fields less than five times the critical field), $\lambda/\mathrm{erf}\lambda\cong 1$. Hence at $x=0$,

$$j\cong\frac{(H_0-H_c)}{4\pi x'}\frac{2}{\sqrt{\pi}}, \tag{12}$$

and at $x=x'$

$$j\cong\frac{(H_0-H_c)}{4\pi x'}\frac{2}{\sqrt{\pi}}\exp(-\lambda^2). \tag{13}$$

An average value for the Joule heat, J, per unit *area* of the moving boundary per unit time is thus

$$J=\frac{\rho}{16\pi^2}\frac{(H_0-H_c)^2}{x'}. \tag{14}$$

This may be rewritten as

$$J=\frac{(H_0-H_c)^2}{8\pi\lambda^2}\dot{x}', \tag{15}$$

in a form comparable to the latent heat per unit area per unit time. If we now treat the Joule heat as if it emanated from the moving boundary, x', we may define an effective latent heat,

$$L'=L-\frac{(H_0-H_c)^2}{8\pi\lambda^2}. \tag{16}$$

For small values of x', the error introduced by this assumption should not be large.

A reiterative procedure may now be employed to incorporate the thermal effects into the electromagnetic propagation equations.

(i) λ is first calculated as a function of H_0, using the equilibrium value for H_c in Eq. (3).

(ii) The boundary temperature depression as a function of H_0 is calculated using λ and the appropriate thermal quantities evaluated at the equilibrium temperature in Eq. (10).

(iii) H_c as a function of H_0 is obtained from a plot of H_c *versus* T.

(iv) Finally, λ as a function of H_0 is recalculated using the corrected value for H_c in step iii. In most instances this process need only be carried through once since subsequent calculations do not significantly alter the results.

[6] The surface temperatures have been arbitrarily set equal to zero to avoid repetitious writing of the constant term.

[7] We make use here of the relationship between x' and t previously obtained from electromagnetic considerations alone.

B. The Infinite Cylinder

The field distribution equation to be solved for the normal phase is

$$\frac{1}{r}\frac{\partial}{\partial r}r\frac{\partial H}{\partial r}-\frac{4\pi}{\rho}\frac{\partial H}{\partial t}=0, \tag{17}$$

where r is radial distance, subject to the boundary conditions:

$$r=r_0,\quad t\geqq 0,\qquad H=H_0,$$
$$r=r',\quad t>0,\qquad H=H_c,$$
$$r=r',\quad t>0,\quad \partial H/\partial r=-4\pi H_c\dot{r}'/\rho.$$

Here r_0 is the outer radius of the cylinder and r' the radius of the interphase boundary. A general solution to this equation is given by

$$H=H_0+\sum_{n=1}^{\infty}A_n\exp\left(-\frac{\rho}{4\pi}\alpha_n^2t\right)J_0(\alpha_nr)+\sum_{n=1}^{\infty}B_n\exp\left(-\frac{\rho}{4\pi}\alpha_n^2t\right)Y_0(\alpha_nr). \tag{18}$$

According to the boundary conditions, the field at the interphase surface must equal the critical value independent of time. It is thus necessary to choose a function, $r(t)$, which will reduce the above equation to an expression independent of time. Unfortunately such a function is not evident.

Faber has attempted to solve the problem by a method of successive approximations. However, his calculations are valid only for values of H_0 close to H_c. At the present time it has not been possible to obtain a general solution to the problem.

C. The Infinite Hollow Cylinder

It is instructive to consider the problem of the hollow cylinder by comparing the solutions to the magnetic propagation equations for the completely normal semi-infinite solid and the infinite cylinder. In the special case that r/r_0 is not too small, the solution for the cylinder may be expanded asymptotically into a form which, at the limit as r approaches r_0, becomes identical with the solution for the semi-infinite solid.[8] It is thus possible to use the equations for the semi-infinite solid to describe the propagation in a thin-walled hollow cylinder. The experimental measurements reported in this paper were made with hollow tantalum cylinders in which $r/r_0\geqq 0.85$.

It is possible, with a hollow cylinder, to measure the resistivity in the normal state in the interval during which the entire cylinder has been driven normal and the field has not yet reached its final equilibrium value. During this period the field, H_i, inside the cylinder, is given implicitly by

$$\left.\frac{\partial H}{\partial r}\right|_{r=r_i}=\frac{2\pi r_i}{\rho}\left(\frac{\partial H_i}{\partial t}\right), \tag{19}$$

where H is the field within the cylinder wall and r_i is the inner radius of the hollow cylinder. Consequently

$$\frac{\partial H_i}{\partial t}=-\sum_{n=1}^{\infty}\frac{\rho}{4\pi}\alpha_n^2[A_nJ_0(\alpha_nr_i)-B_nY_0(\alpha_nr_i)]\exp\left(-\frac{\rho\alpha_n^2t}{4\pi}\right), \tag{20}$$

where α_n are the roots of the equation obtained from the requirement that A_n and B_n be mathematically nontrivial solutions of the simultaneous equations specified by the boundary conditions, i.e., α_n are the roots of

$$2[J_0(\alpha_nr_0)Y_1(\alpha_nr_i)-J_1(\alpha_nr_i)Y_0(\alpha_nr_0)]+\alpha_nr_i[J_0(\alpha_nr_0)Y_0(\alpha_nr_i)-J_0(\alpha_nr_i)Y_0(\alpha_nr_0)]=0. \tag{21}$$

For time intervals such that the quantity $\rho\alpha_1^2t/4\pi>1$, only the first term in the series expansion for the internal field is important. Under this condition the rate of change of field is proportional to $\exp(-\rho\alpha_1^2t/4\pi)$. Since α_1 is determined by the cylinder dimensions, the measured time rate of field increase may be used to calculate the cylinder resistivity.

III. EXPERIMENTAL METHOD

Thin hollow tantalum tubes[9] with an outer diameter of 0.0635 cm and a wall thickness of 0.0047 cm were used as superconducting cylinders. All specimens were initially heated intermittently in vacuum ($<10^{-7}$ mm Hg) at 2800°C until no further rise in system pressure was evident during a ten-second heating cycle.

The resistivity and critical fields of each cylinder were measured under isothermal conditions using standard direct current techniques. The resistivity was also calculated from measurements of the field buildup in the specimen in the manner previously described. The resistivities measured by the two methods were, within the experimental error of several percent, identical.

It was possible to control to some extent the low-temperature resistivity of a specimen by controlling the duration of the heat treating process. The ratio of resistivity at helium temperature to that at room temperature could be varied from a maximum of 0.15 to a minimum of about 0.0045, the latter corresponding to relatively pure tantalum. Since the sharpness of the magnetically induced transition increased with increasing specimen purity, most transition measurements were made on low-resistivity specimens. For these

[8] The error introduced by this procedure is roughly proportional to the quantity $[1-(r/r_0)^{\frac{1}{2}}]$.

[9] Obtained from Superior Tubing Company, Norristown, Pennsylvania.

specimens the critical temperature was approximately 4.46°K, and dH_c/dT at T_c was 320 oersteds/°K.

The driving field was supplied by a niobium coil of 100 turns per centimeter into which the sample could be coaxially inserted. A constant current pulse was produced by discharging into the drive coil and a terminating series resistor 1000 feet of coaxial cable previously charged to an appropriate voltage.

The field inside the cylinder was detected with a small coil whose outer diameter was 0.038 cm and which consisted of 100 turns of number 47 AWG copper wire. Both the drive coil and sense coil lines were coaxially shielded and appropriate damping resistors were incorporated to damp the ringing caused by shock excitation of the output circuit.

Figure 1 is a photograph of the oscilloscope trace of the output of the sense coil following the application of a constant current pulse to the drive coil. The slope in the leading edge of the pulse associated with flux buildup in the sense coil is caused by variations in the cylinder wall thickness. This variation was evident in visual inspection of the cylinders. As would be expected, the ratio of the times measured from $t=0$ to the summit and base of the leading edge are constant for a given cylinder. Since the time required for the field to penetrate the cylinder wall varies with the square of the wall thickness, exceptionally uniform walls are necessary to obtain sharp wave forms. Measurements of the penetration time were made by extrapolating the leading edge of the pulse to the base line and measuring the time from $t=0$ to the intercept. The penetration time so obtained corresponds essentially to the minimum wall thickness.

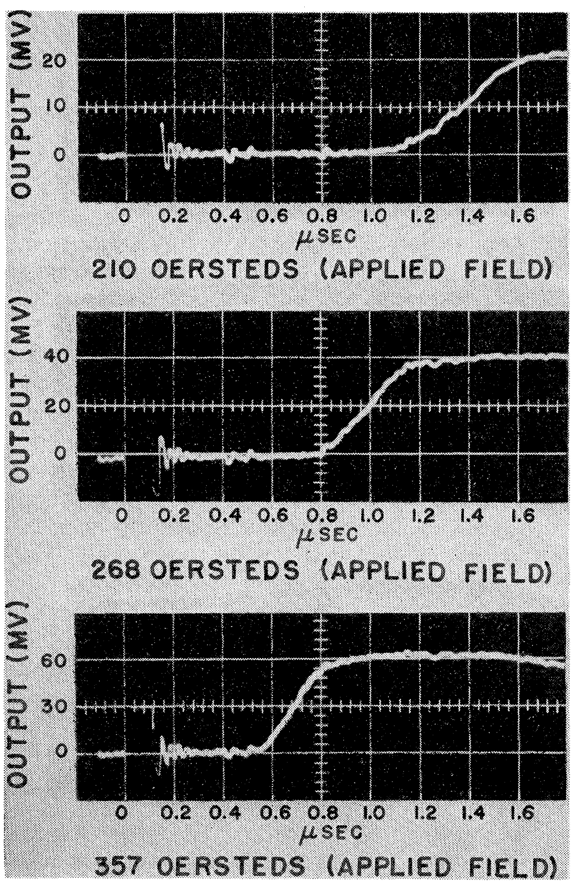

FIG. 1. Sense coil output voltage following the application of a constant current pulse to the drive coil. Sweep speed is 0.2 microsecond per cm; drive fields from top to bottom of 210, 268, and 357 oersteds.

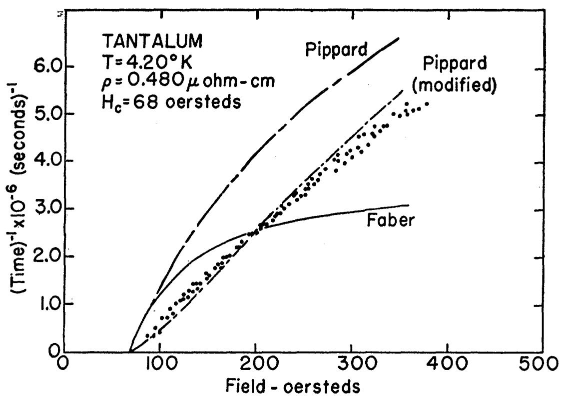

FIG. 2. Inverse of the penetration time for several series of measurements, plotted as a function of the driving field for a relatively impure tantalum sample, compared with theoretical calculations.

IV. RESULTS

Measurements of the penetration time for two tantalum cylinders in a bath at 4.2°K are plotted in Figs. 2 and 3. For convenience the reciprocal of the penetration time has been plotted as a function of the driving field. The plotted curves indicate the results which are predicted according to the equations given by Pippard and Faber, and the results which are predicted by modifying Pippard's treatment to include thermal corrections. In obtaining the desired thermal corrections, values for the thermal conductivities were taken from the work of Hulm,[10] values for the specific heat from the data of Worley *et al.*[11] The latent heat was calculated from direct measurements of the temperature, the critical field, and of the variation of the critical field with temperature.

Figure 4 contains experimental points for the penetration time obtained at a number of bath temperatures. The curves correspond to the theoretical predictions obtained by including thermal effects. In all cases it is apparent that the experimental results are in good agreement with the theoretical predictions.

The results with tantalum are in marked contrast to the results obtained by Faber with tin cylinders, in which thermal effects were found to be negligible. In

[10] J. K. Hulm, Proc. Roy. Soc. (London) **A204**, 98 (1950).
[11] Worley, Zemansky, and Boorse, Phys. Rev. **91**, 1567 (1953).

tantalum the ratio of the electrical resistivity to the thermal conductivity is several thousand times as large as the corresponding ratio in even relatively impure tin specimens. In tin, therefore, the thermal conductivity is sufficiently high and the rate of phase propagation sufficiently low that the specimen temperature remains uniform during the transition. In tantalum this is not the case.

As the transition rates are increased through the use of larger driving fields, time delays which may be associated with the time required to form a nucleus of normal material within the specimen might be expected to make themselves evident. Within the limits of error associated with the present measurements no such effects have been observed.

It should also be pointed out that flux trapping was not observed in any of the tantalum specimens used for this work. Indeed, oscilloscope traces of the sense coil voltage following the termination of the drive pulse indicated that the flux emerged from the specimen at a rate corresponding to that expected for a completely normal cylinder. Faber has observed a similar phenomenon in tin, and has discussed several possible mechanisms which might prevent flux trapping. He suggests such mechanisms as the inability of the ends of a superconducting sheath to coalesce due to the surface free energy, and the ability of a closed sheath to migrate to the specimen surface. There exists the further possibility, in tantalum, that the eddy current heating following the phase transition[12] may heat the specimen above its critical temperature. Flux leaving the specimen would produce eddy currents sufficient to maintain the temperature long enough to prevent flux trapping.

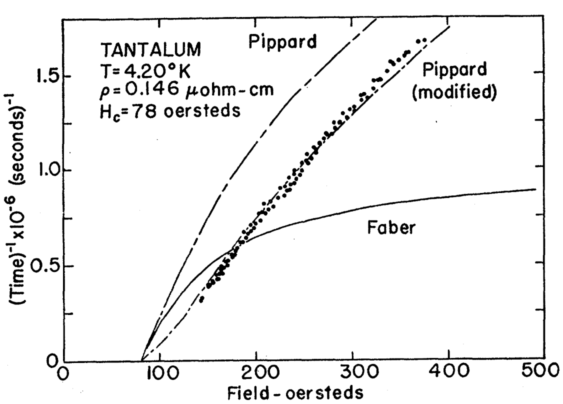

FIG. 3. Inverse of the penetration time for several series of measurements, plotted as a function of the driving field for a moderately pure tantalum sample, compared with theoretical calculations.

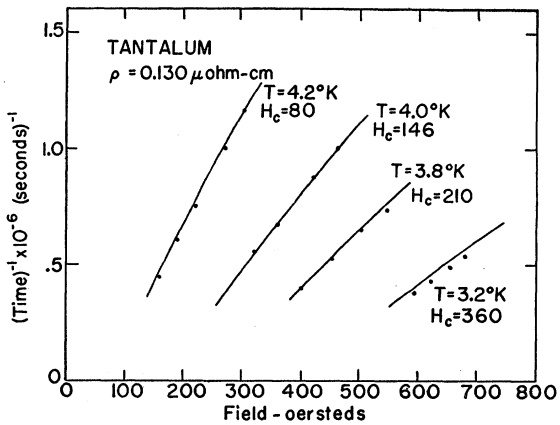

FIG. 4. Inverse of the penetration time *versus* driving field for several different bath temperatures. The solid lines represent the results calculated according to the method outlined in the text.

The foregoing work supports Pippard's hypothesis that the time rate of propagation of the normal phase in a superconducting body is determined by the eddy current damping which accompanies the spatial propagation of the normal phase. For materials like tantalum, in which the ratio of normal resistivity to thermal conductivity is high, the transition is not an isothermal process and thermodynamic considerations must be incorporated to describe adequately the observed effects. The time required for the normal phase to propagate a given distance decreases monotonically with the driving field, and does not approach a limiting value as might be inferred from the smaller field calculations used by Faber.

ACKNOWLEDGMENTS

The author would like to express his appreciation to Dr. D. R. Young, Dr. J. I. Budnick, and Mr. M. E. Drougard for many helpful and stimulating discussions during the course of this work.

[12] For the experiments described here, the time required to drive the specimen into the normal state is small compared to the time required for the magnetic field to reach equilibrium throughout the normal specimen. Eddy current heat is generated whenever the magnetic field is not in equilibrium, while latent heat is liberated or absorbed only during the period when a phase change is taking place.

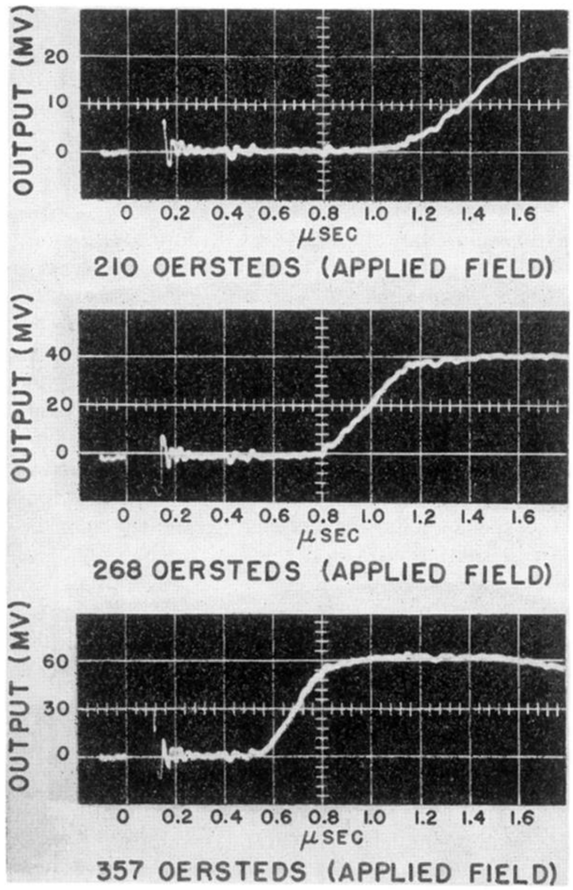

FIG. 1. Sense coil output voltage following the application of a constant current pulse to the drive coil. Sweep speed is 0.2 microsecond per cm; drive fields from top to bottom of 210, 268, and 357 oersteds.